International Journal of Heat and Mass Transfer 51 (2008) 5598–5609

Contents lists available at ScienceDirect

International Journal of Heat and Mass Transfer

journal homepage: www.elsevier.com/locate/ijhmt

Computational modeling of intravitreal drug delivery in the vitreous chamber with different vitreous substitutes

Jyoti Kathawate, Sumanta Acharya *

Mechanical Engineering Department, Louisiana State University, Room 1419B, CEBA, Baton Rouge, LA 70803-6413, United States

ARTICLE INFO

Article history:
Received 15 November 2007
Received in revised form 4 April 2008
Available online 23 July 2008

ABSTRACT

Intravitreal injection of drug is commonly used to treat vitreoretinal diseases. In order to assess the effectiveness of the injected drug, it is critical to know the drug distribution within the eye following the injection. This is particularly important when the vitreous medium has been replaced by fluid substitutes. The main objective of this paper is to characterize the spatio-temporal evolution of drug distribution following intravitreal injection into a vitreous substitute such as silicone oil. In addition, water is considered as an intravitreal fluid to represent the liquefaction of vitreous that occurs with aging. Both direct injection of drugs and injection of time-released drugs are studied. The results show that the concentration distribution depends on the properties of the vitreous substitute, the diffusion coefficient of the drug and the permeability of the retinal surface. For drugs with high diffusion coefficients, convection plays a small role in the drug transport. For drugs with low diffusion coefficients and in low viscosity vitreous fluids, convection is seen to play a more important role and can lead to high drug concentrations on the retina which can be potentially toxic. Time-released drug injection is shown to avoid conditions of retinal toxicity, and to provide lower drug concentrations with sustained residence times along the retinal surface. For drugs with high diffusivity and retinal permeability, uniform distribution of the drug is obtained along the surface of the retina, while for drugs with low diffusion coefficient and retinal permeability the concentration of drug is localized along the posterior surface of the retina.

1. Introduction

The treatment of retinal diseases is currently limited by the difficulty in delivering effective doses of the drugs to target tissues in the vitreous chamber of the eye (Fig. 1a). Many drugs have a narrow concentration window of effectiveness and may be toxic at higher concentrations. Therefore, the ability to predict local drug concentration is critical for proper drug delivery. An intravitreal injection provides the most direct approach to delivering drugs to the tissues in the vitreous segment. However, intravitreal injections have potential side effects of retinal detachment, hemorrhage, endophthalmitis, and cataract [1]. In many cases, repeated injections are needed to maintain the effective range of drug concentrations for a certain period of time since the half-life of drugs in the vitreous is relatively short. Repeated injections cause patient discomfort and may further lead to complications such as vitreous hemorrhage, infection, and lens or retinal injury [2]. Therefore, an understanding of the transport of different drugs following intravitreal injection is necessary, so that, the most effective utilization results from each injection. In the present study, a time-dependent numerical model for studying drug transport following intravitreal injection is developed with the goal of understanding the important parameters that play a critical role in the drug distribution in the presence of vitreous substitutes.

A few recent studies have examined the transport of drugs injected in the vitreous chamber. Araie and Maurice [3] measured the distribution contours of fluorescein and fluorescein glucuronide in the rabbit vitreous by freezing the eyeball and sectioning it. Fitting the experimental data with a diffusion model, they obtained the permeability values of the retinal-blood barrier for different solutes. Tojo and Ohtori [4] assumed that the vitreous body was a part of a cylinder and the surface was divided into three areas, characterized by the drug-elimination pathways: the retina-choroid membrane, the lens, and the hylaoid membrane. They developed a general mathematical model based on Fick's second law of diffusion describing the pharmacokinetics of the intravitreal injection of dexamethasone sodium *m*-sulfobenzonate (DMSB). Friedich et al. [5,6] used a finite element analysis to solve the diffusion-only, mass transfer problem in the stagnant vitreous humor. They studied the effects of different parameters that affect the concentration distribution in the vitreous humor.

Controlled release of a therapeutic agent from a time-released polymeric system presents an improvement to traditional direct injection treatment strategies and it can overcome some of the problems associated with direct drug delivery. Controlled drug delivery systems are designed for long-term administration in which the drug level remains constant, between the desired

* Corresponding author. Tel.: +1 225 578 5809; fax: +1 255 578 5924.
E-mail address: acharya@me.LSC.edu (S. Acharya).

0017-9310/$ - see front matter © 2008 Elsevier Ltd. All rights reserved.
doi:10.1016/j.ijheatmasstransfer.2008.04.053

Nomenclature

c	local concentration of the drug
C_2	inertial resistance factor
D	diffusion coefficient of the drug
D_p	characteristic size of the solid portion in the porous region, Eq. (6)
k	rate constant of drug release, Eq. (1)
M	initial loading of the drug injected, Eq. (1)
P	pressure in the eye
q	source term in the species transport equation representing drug release, Eq. (1)
t	time
Sc	Schmidt number, $\frac{\mu}{\rho D}$
$\vec{v}$	velocity vector
V	volume, Eq. (1)

Greek symbols

α	permeability, Eq. (5)
μ	viscosity
ρ	density
ε	void fraction in the porous regions, Eq. (6)

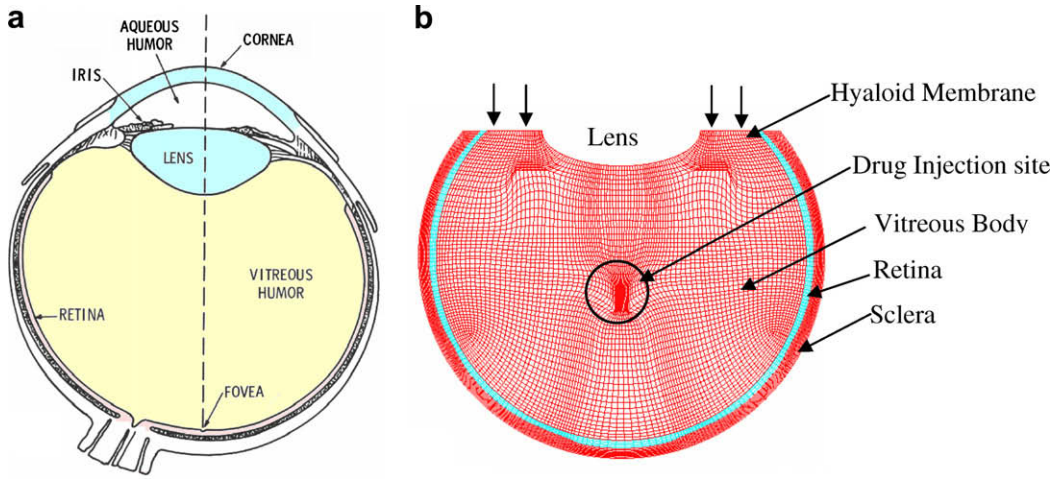

Fig. 1. (a) Cross-section of the human eye [15], (b) computational grid.

maximum and minimum level, for an extended period of time. Xu [7] developed a two-dimensional convection–diffusion transport model of the drug released from a cylindrical local source in a vitreous modeled as a porous media. Stay et al. [8] developed a three-dimensional transport model of the drug following intravitreal injection from a point source. Missel [9] studied bolus injection and drug delivery from intravitreal devices for a rabbit eye model. In all these studies, the convection driven by the pressure drop across the vitreous was taken into account, but with a porous media model for the vitreous. Park et al. [10] developed a three-dimensional finite element method to simulate the pharmacokinetics in the entire rabbit eye following the drug administration by intravitreal injection through a controlled release implant. All the studies reported above have assumed that the working fluid is the vitreous humor for which a porous media approximation is reasonable.

One of the more recent developments in eye surgery has been the introduction of the surgical procedure called vitrectomy. Trans-pars-plana vitrectomy (TPPV) is used to treat many different retinal disorders such as proliferative diabetic retinopathy (including vitreous hemorrhage), macular hole formation, and intraocular infections (endophthalmitis). In TPPV, the vitreous is removed and replaced with a vitreous fluid substitute. Silicone oil, fluorosilicone oil, and perfluorocarbon liquid are among the most commonly used vitreous substitutes [11]. Retinal tears are often associated with age-related liquefaction and shrinkage of the vitreous body. In these cases, the vitreous substitutes can be used intra-operatively to push a detached retina to its normal position and to restore the volume of the vitreous cavity. When the drug is injected into the vitreous cavity, knowledge of the drug distribution following injection is very important in order to maximize the therapeutic benefits while minimizing damage to the tissues due to high local concentration. This is highlighted by a study by Stainer et al. [12] and Hegazy et al. 013] who have shown that the concentration of drug that is non-toxic when injected into a normal eye can be toxic if used to treat a vitrectomised eye. Thus, it can be potentially dangerous to use the knowledge base for a normal eye to treat the vitrectomised eye, and it is important to develop an understanding of the drug transport with vitreous substitutes.

The goal of the present work is to simulate intravitreal drug delivery in the presence of vitreous substitutes. As discussed above, there is limited information available on intravitreal drug distribution in the normal eye and is based on the studies carried out in [5–10]. However, there is no information available on how the drug is transported in the presence of vitreous substitutes that have different transport properties. In the present study, silicone oil is considered as the vitreous substitute. Both direct injection of drugs and injection of a time-released drug (that, in actual practice, is encapsulated in a bio-degradable polymer) are studied.

Another problem associated with the vitreous is the liquefaction of the vitreous humor [2]. With aging (>45–50 years), the volume of the vitreous-gel in the human eyes decreases steadily, and the volume of the liquid portion of the vitreous proportionally increases [14]. Thus, due to vitreous liquefaction with time, fluid circulation is expected in the vitreous chamber leading to a reduction of gradients in the drug concentration within the liquefied portion. This will lead to the reduced half-life of the drug in the vitreous chamber [2]. Therefore, in the present study, we have also included

water as one of the vitreous fluids in order to compute the drug transport for the case of liquefied vitreous.

2. Mathematical model

2.1. Geometrical model of posterior segment of human eye

The geometrical model adopted in the present study, shown in Fig. 1b, is based on the physiological dimensions of a human eye provided by L'Huillier et al. [15]. The vitreous chamber is mainly composed of vitreous humor and comprises about two-third of the eye with a volume of approximately 4 mL [16]. The viscous properties of the vitreous humor allow the eye to return to its normal shape if compressed. The crystalline lens is located just behind the iris and is modeled here as a stationary ellipsoid of 4 mm diameter along the anterior–posterior axis and 9 mm diameter along the two other axes. The hyaloid membrane is composed of loosely packed collagen fibers and hyaluronic acid, and spans the gap between the lens and the ciliary body. Although the hyaloid membrane forms a boundary between the nearly stagnant vitreous and the flowing aqueous humor, it does not form a limiting boundary to the transport of small molecules such as fluorescein. The retina is a light-sensitive layer at the back of the eye that covers about 65 percent of its interior surface and is immediately adjacent to the vitreous. The retina is a remarkably fragile tissue, having a thickness of 250 μm [17] and is modeled here as a sphere with a radius of 9.1 mm. The distance between the lens and retina centre is 5 mm. The choroid lies between the retina and the sclera. It is composed of layers of blood vessels that nourish the back of the eye. The sclera is commonly known as "the white of the eye." It is the tough, opaque tissue that serves as the eye's protective outer coat. The average thickness of sclera is assumed to be 0.065 cm in the present work as reported in [16].

2.2. Drug delivery model

The traditional approach of drug delivery is the direct injection of the drug in a solution form. More recently, micro-spheres of biodegradable polymer such as poly (lactic acid) have been used as drug carriers. The micro-spheres of poly (lactic acid) are resolved into monomers of lactic acid by hydrolytic deesterification before they finally disappear. In this study, we have explored both these approaches of drug delivery, i.e., (i) direct injection where the injected drug is instantaneously released from a specified volume and (ii) time-released drug injection where the drug is released as a function of time. There are many parameters that potentially control how the drug is initially distributed in the vitreous chamber which include: needle gauge, needle length, penetration angle of the needle, speed of the injection, rheology of the injected solution, and rheology of the vitreous. Numerical analysis carried out by Friedrich et al. [5] showed that the results obtained by modeling the initial drug injection site as a cylinder or a sphere were identical. Therefore, in the present study we have assumed that the drug is released at the center of the vitreous chamber and that the injected drug initially has a homogenous distribution within a cylindrical region after injection. The initial size of the cylindrical region was assumed to be 0.075 cm in diameter and 0.15 cm in height [7]. The density of the drug is assumed to be same as that of water i.e., 1000 kg/m^3. The initial normalized mass fraction of the drug is assumed to be 1 (normalized with respect to the concentration of the drug in the water base) within the domain of the drug injection site while it is 0 in rest of the vitreous.

The diffusivity of small molecules, such as gentamicin, fluorescein and fluorescein glucuronide in the vitreous humor was found experimentally by Araie et al. [3] and Kaiser et al. [18] to be 6e−10 m^2/s, whereas for larger molecule drugs such as FITC-Dextran, the diffusivity is found to be 3.9e−11 m^2/s [19]. Further, for very large molecules e.g., an antibody, the diffusivity is lower and is of the order of 1e−11 m^2/s [8]. Therefore, for the current study we have considered three possible diffusion coefficients for the drugs, i.e., 6e−10 m^2/s, 3.9e−11 m^2/s and 1e−11 m^2/s. There is no published data that provides the diffusion coefficient of drug in vitreous substitutes. Rashidnia et al. [20] using interferometric measurements and the Wiener model calculated the diffusion coefficient of silicone oil with different kinematic viscosities. They report that the diffusion coefficient of 1 cSt oil (viscosity comparable to water) in 1000 cSt silicone oil to be 2.48e−10 m^2/s (indicating that diffusion coefficients in silicone oil are of comparable magnitudes as that reported in literature [3,8,18]). In the absence of quantitative information about the diffusion coefficient of drug with silicone oil, a range of values are chosen, we have considered five possible diffusion coefficients for the drugs (i.e., 6e−10 m^2/s, 3.9e−11 m^2/s and 1e−11 m^2/s, 6e−12 m^2/s and 1e−12 m^2/s), so that the results can be used to evaluate the role of the diffusion coefficients within an order of magnitude variation (from e−10 to e−12).

For time-released drug injection, since we are interested in controlling the drug delivery release rate, we have modeled the source term in the scalar concentration with the following volumetric release rate of the drug,

$$q = \frac{M * k}{V * \sqrt{t}} \tag{1}$$

where M is the initial loading of the drug (kg), k is the rate constant of the release (s^{-1}) and V is the volume of the drug injection (m^3). The source term above is defined only at the injection site and is zero for all other positions within the vitreous. In earlier studies by Falk et al. [21], who studied the release of gentamicin from poly-(ι-lactic) micro-spheres in cadaveric bovine vitreous, the value of k was taken to be 0.057 day$^{1/2}$ and the initial mass of the drug M was assumed to be 795 μg.

3. Numerical details

3.1. Grid generation

The three-dimensional geometry of the human eye is generated using the commercial software Grid-Pro. A structured multi-block mesh with 541,250 hexahedral cells of aspect ratio less than three are used in the computational domain. The entire geometry is divided into 922 blocks with 5 blocks representing the drug injection position. The retina and the choroid-sclera are modeled as two different layers with different hydraulic conductivity. As described earlier, the drug is released at the center of the vitreous chamber and is assumed be cylindrical in shape at $t = 0$. The drug injection position is shown encircled in Fig. 1b. As the drug injection site is very small the grid is refined in the drug injection region.

3.2. Boundary conditions

The hyaloid membrane separates the vitreous humor from the aqueous humor and the anterior segment of the eye. Therefore, we have considered pressure at the hyaloid membrane to be same as that of aqueous humor, which is close to the intraocular pressure of the eye. Normal IOP ranges between 15 and 20 mmHg (∼2000–2666 Pa). In the present study, we have assumed the pressure at the hyaloid membrane to be 2000 Pa. As in [7,8], the concentration is set to zero i.e., $C = 0$ at the hyaloid membrane. This boundary condition is based on the assumption that the aqueous flow rate is high relative to the release of the drug. The lens is

assumed to be impermeable to both flow and the drug concentration. Therefore, at the surface of the lens a no-flux boundary condition is applied. The retina and the sclera are treated as two different layers and each layer is treated as a porous zone with their respective permeability. In the present work, permeability values from the literature are used for the retina and the sclera. Drugs with small molecules have higher retinal permeability, whereas the drugs with large molecules have lower retinal permeability. It is shown by Friedrich et al. [5] that retinal permeability plays a very important role in drug distribution. For small molecule drugs where $D = 6e{-}10\ m^2/s$ the retinal permeability values reported by Araie [3] 2.33e−5 cm/s is used, while for large molecule drugs where $D = 3.9e{-}11\ m^2/s$ the retinal permeability value reported by Pitkänen [19] 1e−8 cm/s is used. For the sclera, which is a dense connective tissue, Ethier et al. [22] reported a permeability value of 1.96e−9 cm/s and the pressure along this surface is assumed to be the normal venous pressure, i.e., 1200 Pa. The choroid layer, which is situated outside the retina, is highly vascularized; therefore, a reasonable assumption is that choroid will act as a perfect sink for drug transport across the retina. Therefore, at the outer surface of the retina the drug concentration is set to zero i.e., $C = 0$ [5,6].

3.3. Material properties

The most widely used vitreous substitutes is silicone oil [23]. Silicone oil has low density compared to water which causes it to float upon the residual fluid and thus helps in retinal tamponade in the case of superior breaks. As seen in Table 1, silicone oil has higher viscosity compared to water (approximately three orders higher in magnitude). As noted earlier, we will use water and silicone oil as the two vitreous fluids of interest.

3.4. Governing equations

The complete three-dimensional incompressible Navier–Stokes equations along with species transport equation are solved to obtain the velocity, pressure and concentration fields.

Continuity equation:

$$\frac{\partial \rho}{\partial t} + \nabla \cdot (\rho \vec{v}) = 0 \tag{2}$$

Momentum equations:

$$\frac{\partial \vec{v}}{\partial t} + (\vec{v} \cdot \nabla)\vec{v} = -\frac{1}{\rho}\nabla P + \frac{\mu}{\rho}\nabla^2 \vec{v} + \vec{g} \tag{3}$$

Species transport equation:

$$\frac{\partial c}{\partial t} + \vec{v} \cdot \nabla c - D\nabla^2 c - q = 0 \tag{4}$$

where P is the pressure, c is the concentration of the drug, D is the diffusion coefficient and q is the release rate as a function of position and time. The source term q is modeled using Eq. (1).

Porous media is modeled by the addition of a momentum source term to the standard fluid flow equations. The source term is composed of two parts: a viscous loss term and an inertial loss term. To model the porous region of the retina and the sclera, the ∇P term in the momentum equation, Eq. (2), is represented by the following equation:

$$\nabla P = \frac{\mu}{\alpha} V_i + C_2 \frac{\rho}{2} |V_i| V_i \tag{5}$$

where α is the permeability and C_2 is the inertial resistance factor. To get appropriate values of constant α and C_2, a semi-empirical correlation, derived from the Ergun equation [24], is used. These correlations for the permeability α and inertial resistance factor C_2 are applicable over a wide range of Reynolds number and for various packing levels, and are given as

$$\alpha = \frac{D_p^2 \varepsilon^3}{150(1-\varepsilon)^2}, \quad C_2 = \frac{3.5(1-\varepsilon)}{D_p \varepsilon^3} \tag{6}$$

where D_p is the mean particle diameter of the packed bed and ε is the void fraction. Void fraction is defined as the volume of voids divided by the volume of the packed bed region. The sclera consists of 89.7% of water and 7.75% of collagen and glycosaminoglycans (GAG's) [25], which causes an increase in the resistance. Based on the data in [26] the void fraction for sclera was considered to be 0.91 and $D_p = 1.35\ \mu m$. These values of ε and D_p lead to specific hydraulic permeability of $2e{-}18\ m^2$ for sclera which is consistent with those reported by Ethier et al. [22] for the sclera. For small molecule drugs where $D = 6e{-}10\ m^2/s$ the retinal hydraulic conductivity is 2.6e−5 cm/s [3] and for large molecule drugs where $D = 3.9e{-}11\ m^2/s$ the retinal hydraulic conductivity is 1e−8 cm/s [19]. The void fraction of retina is taken to be $\varepsilon = 0.6$ as provided in [16]. Using Eq. (6), for small molecule drugs D_p is calculated to be 1.71e−6 m and for large molecule drugs D_p is calculated to be 3.36e−8 m. These values lead to a specific hydraulic permeability value of $2.65e{-}14\ m^2$ and $1.019e{-}17\ m^2$ respectively.

3.5. Computer code

The commercial code FLUENT [27] is used in this study. This code is based on a control-volume approach where the computational domain is divided into a number of cells, and the governing equations are discretized into algebraic equations in each cell. The control-volume approach leads to a discretized set of equations which satisfies the integral conservation of the mass and the momentum over each control volume. For solving the system of algebraic equations, a Gauss–Siedel scheme is used. Although the Gauss–Siedel scheme rapidly removes the high frequency errors in the solution, low frequency errors are reduced at a rate inversely related to the grid size. A W-cycle multi-grid scheme is used to accelerate the convergence rate by applying corrections to coarser grid levels. The coupling between velocity and pressure is handled using the SIMPLEC-algorithm [28], which uses the conservation of mass equation to derive a pressure corrector equation, and uses a pressure and velocity correction step to yield continuity satisfying velocity fields at each iteration. The pressure and velocities are then corrected so as to satisfy the continuity constraint. The discrete values of the variables are stored at the cell-centers, but the convection terms in the discretized equation must be interpolated at the cell faces from the cell-center values. A second order upwind scheme is used for deriving the face values of different variables in the momentum equation. For the pressure Poisson equation, a second order accurate discretization scheme is used.

Table 1
Material properties of the vitreous substitutes

Vitreous substitute	Density (kg/m^3)	Viscosity (kg/ms)
Water	1000	0.001
Silicone oil	970	1.067

4. Results and discussion

4.1. Grid independence study and validation

To demonstrate grid independence, simulations are run with 541,250 cells and 1,121,000 cells. As seen in Fig. 2, less than 1%

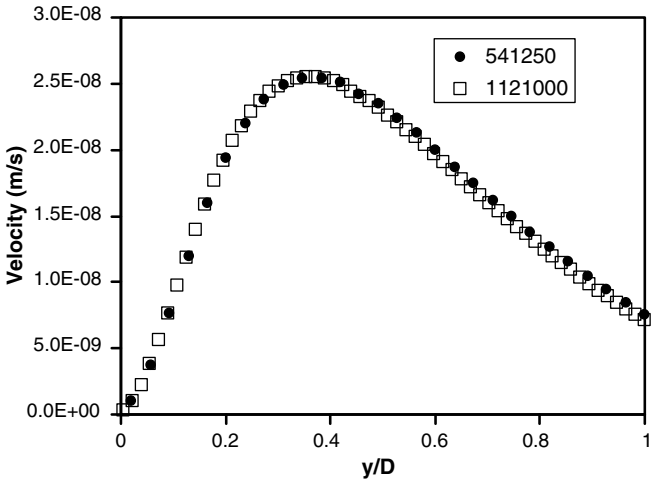

Fig. 2. Velocity magnitude along the center of vitreous chamber for 541,250 and 1,121,000 hexahedral cells.

variation in the magnitude of the maximum velocity is observed between the calculation on the two grids. This good agreement between the solutions from the two grid levels justifies the use of 541,250 cells for the simulation.

As a further validation of the numerical model, the results are compared with the predictions of Friedrich et al. [29] who carried out a finite element analysis to predict the concentration of injected at different locations in vitreous chamber for phakic and aphakic eyes. In the study carried out by Friedrich et al. [29], vitreous was assumed to be stagnant, i.e., effects of convection were neglected. The permeability of retinal surface is considered to be 1e−7 cm/s and the drug injection volume is considered to be 15 μL. For the present validation, the central injection case was considered and the diffusion coefficient of drug was considered to be 5.6e−10 m^2/s [29]. Fig. 3a shows the concentration contours for the half section of the vitreous chamber for the current model. As seen in Fig. 3b, the current prediction of the concentration along the center of vitreous chamber agrees well with Friedrich et al. [29].

4.2. Pressure and velocity fields

The first step in the simulation process was the determination of the pressure and the velocity profiles within the vitreous at steady state. The liquid vitreous case was compared with the predictions in which vitreous was modeled as a porous medium as in Xu [7]. In the case of vitrectomy, as mentioned above, the vitreous is removed completely along with the collagen fibers and is replaced with different vitreous substitutes. Therefore, for these cases the vitreous cannot be modeled as a porous medium and has to be treated as a liquid.

4.2.1. Pressure contour

Fig. 4a shows the pressure distribution for the cases where the vitreous is modeled as a porous medium and Fig. 4b shows the corresponding pressure distribution with the vitreous modeled as a fluid (water). The higher pressure specified at the hyaloid membrane (2000 Pa) drives the aqueous from the hyaloid to the sclera which is maintained at a venous pressure of 1200 Pa. When the vitreous is considered as a porous medium, there is a pressure drop of about 180 Pa across the vitreous humor. These results are consistent with the earlier results obtained by Xu [7]. In the case of a liquid vitreous, as seen in Fig. 4b, the vitreous humor is at a uniform pressure of 2000 Pa and the pressure drop essentially occurs across the retinal and the scleral tissues. This implies that the entire retina and the lens are at higher pressure relative to the porous media case. These higher pressures on the lens surface may be responsible for the reported cataract complications occurring after vitrectomy [23,31].

4.2.2. Velocity contour

Fig. 5 shows the predicted fluid velocity profile within the vitreous chamber for water and silicone oil as vitreous substitutes. Velocity magnitudes in the posterior segment are very low and are smaller than 0.009 μm/s. However, as shown later, for low diffusivity drugs, convective effects can be important. Therefore, it is important to study the behavior of the flow distribution within the vitreous chamber.

Fig. 5a and b shows the path-lines superimposed on the velocity magnitude contour for the porous media vitreous and the liquid vitreous respectively. The path-lines for both the cases are nearly identical with the flow directed from the hyaloid membrane to the retinal surface. The velocity magnitudes are lower for the porous medium due to higher flow resistance and appear to have a flatter distribution in the *x*-direction. Fig. 5c and d show the velocity magnitude along the center-line of the vitreous chamber. The peak velocity location in the case of porous medium is shifted upwards towards the lens compared to the cases with vitreous fluids since the porous medium acts as a momentum sink and rapidly decelerates the flow. When compared to the case of water as vitreous substitute, it is seen that there is a 25% decrease in the peak velocity with the porous medium. Silicone oil has higher dynamic viscosity compared to water (approximately order of 1000 higher), as a result of which, silicone oil has considerably lower velocity (approximately order of 1000 lower) compared to the other two cases. As seen later, this huge variation in velocity plays a major role in the drug distribution within the vitreous chamber.

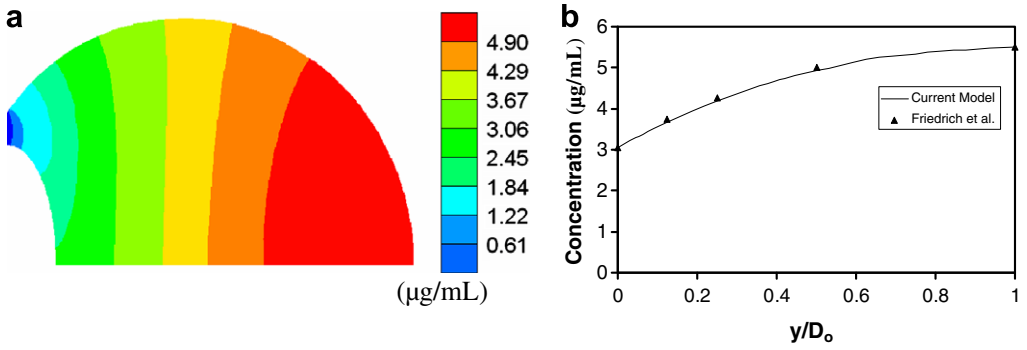

Fig. 3. Concentration contours: (a) current model, (b) concentration along the center of the vitreous chamber comparison with Friedrich et al. [29].

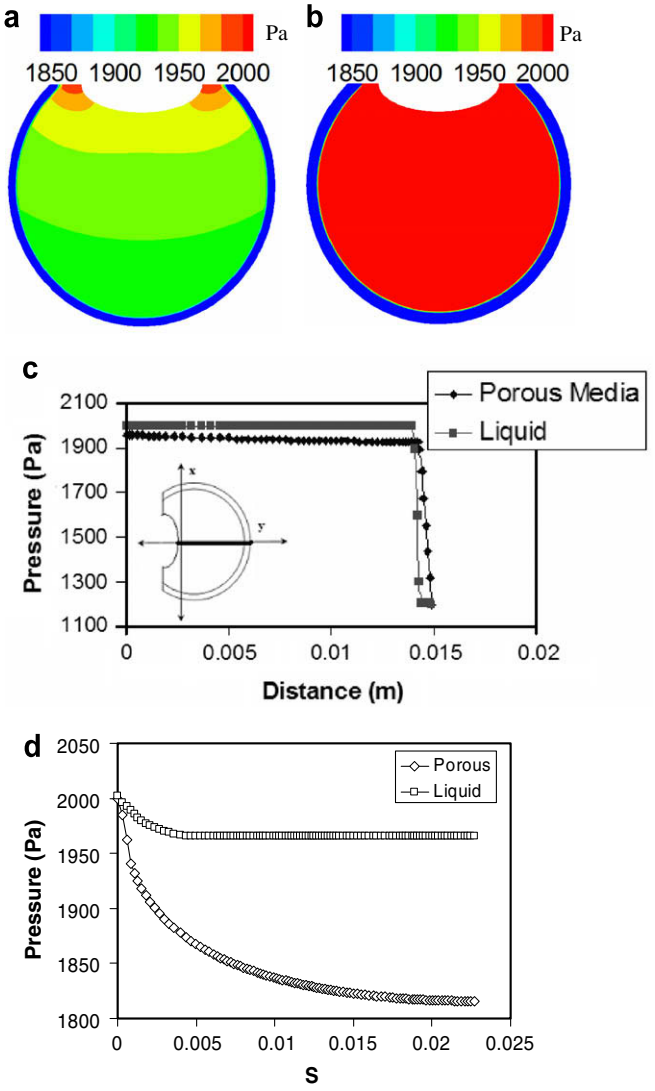

Fig. 4. Pressure contour: (a) vitreous modeled as porous medium, (b) vitreous modeled as liquid (water), (c) pressure plot along the center of the vitreous chamber and (d) along the surface of the retina.

4.3. Concentration distributions

4.3.1. Direct injection

Results will be first presented for the direct injection technique of drug injected into water and silicone oil. With the direct injection technique, the drug is released instantaneously from a pre-defined volume as shown in Fig. 1b. Retinal hydraulic conductivity for small molecule drugs e.g., gentamicin, fluorescein, etc., has been reported to be 2.6e−5 cm/s [3]. Retinal hydraulic conductivity for large molecule drugs e.g., FITC-Dextran has been reported to be 1e−8 cm/s [19]. To analyze the effects of low diffusion coefficient, two different drugs are studied (1) FITC-Dextran with $D = 3.9e{-}11\ m^2/s$ and (2) antibody with $D = 1e{-}11\ m^2/s$. To show the effects of diffusion coefficient, for low diffusion coefficient drugs, the retinal permeability (∼hydraulic conductivity) is fixed and the drug diffusion coefficient is varied.

Fig. 6 shows the contour plots for the concentration of the drug on the central plane of the vitreous chamber at time $t = 100$ h after the drug is released. At this time instance, the drug has reached the retinal surface, and a fraction of the drug has crossed the retinal interface entering the vascular flow in the choroid. Qualitatively, the numerical results obtained by the current model for a human eye are comparable to the experimental results obtained by Araie [3] for a rabbit eye. The results cannot be exactly compared because the volume of rabbit vitreous is 1.46 mL whereas for human eye the volume is 4 mL. For high diffusion coefficient drugs (Fig. 6a and b), diffusional transport is more important, and since diffusion is nearly circumferentially-isotropic ($C = 1$ at the center and 0 along the retinal-choroid circumference), the concentration contour lines are parallel to the retina which implies that the diffusional flux of fluorescein across the retinal surface was the main route of drug elimination. For highly viscous vitreous substitutes like silicone oil, where velocities are lower, the drug is transported across the retinal layer more slowly compared to water. Thus, as seen in Fig. 6b, at $t = 100$ h, a higher amount of drug is still present for the case of silicone oil compared to water where, due to the higher transport rates, a larger fraction of the drug has already crossed the retinal boundaries.

Fig. 6c and d shows the concentration contours of the drugs with a lower diffusion coefficient, $D = 3.9e{-}11\ m^2/s$ (e.g., FITC-Dextran), at time $t = 100$ h after injection. In this case, as the diffusion coefficient of the drug is lower, the diffusive transport of the drug is reduced in the vitreous chamber and convection begins to play a more important role. For low diffusion coefficient drugs, the concentration contour lines are perpendicular to both retina and lens boundaries along their entire length, indicating that the diffusional fluxes across these surfaces are negligible whereas the concentration contour lines are almost parallel to the hyaloid membrane, indicating that the diffusional flux was normal to this tissue. This is in contrast to the higher diffusivity drug case in Fig. 6a and b where the concentration lines are parallel to the retinal surface. Note that since the downward-directed convection begins to play a more important role, drug concentrations are higher along the bottom retinal surface (vicinity of the optic nerve head) and lower in the vicinity of the hylaoid. For the drugs with $D = 1e{-}11\ m^2/s$ (Fig. 6e and f), with the decrease in diffusion coefficient by a factor of four, the drug transport rates are reduced. At this time it is seen that for water (Fig. 6e), most of the drug concentration has reached the lower retinal surface and the concentration levels are low in the upper half of the vitreous chamber. This, in turn, implies that convection plays an important role in the transport process, and nearly all the drug is transported through the lower portion of the retinal surface. In Fig. 6f, it is seen that for the high-viscosity silicone oil, the peak concentration of drug is still at the drug injection site (due to the lower transport rates), and that the iso-concentration lines are circular (indicative of the weaker role of convection).

Fig. 7 shows the concentration plot of the drug at the center of retinal surface with respect to time for water and silicone oil as vitreous fluids. It is seen that, the concentration of the drug reaching the center of retina increases quickly after the injection and then decays as the drug is transported across the surface of the retina. For high diffusion coefficient drugs (Fig. 7a), the drug reaches the maximum concentration at time $t = 4.6$ h which is in agreement with the numerical analysis carried out by Friedrich et al. [6]. For lower diffusivity drugs (Fig. 7b), convection begins to play a more important role. In highly viscous vitreous substitutes like silicone oil, where velocities are lower, the drug is transported across the retinal layer more slowly compared to water. It is seen in Fig. 7b that decreasing the drug diffusivity through the vitreous increases the time required for the drug molecules to travel from the drug injection site to the retinal surface. The concentration of the drug reaching the center of retinal surface increases quickly for drugs with $D = 3.9e{-}11\ m^2/s$ following injection compared to drugs with lower diffusion coefficient $D = 1e{-}11\ m^2/s$, and then decays as the drug is transported across the lower surface of the retina. For drugs with $D = 3.9e{-}11\ m^2/s$, for the case of water, the concentration

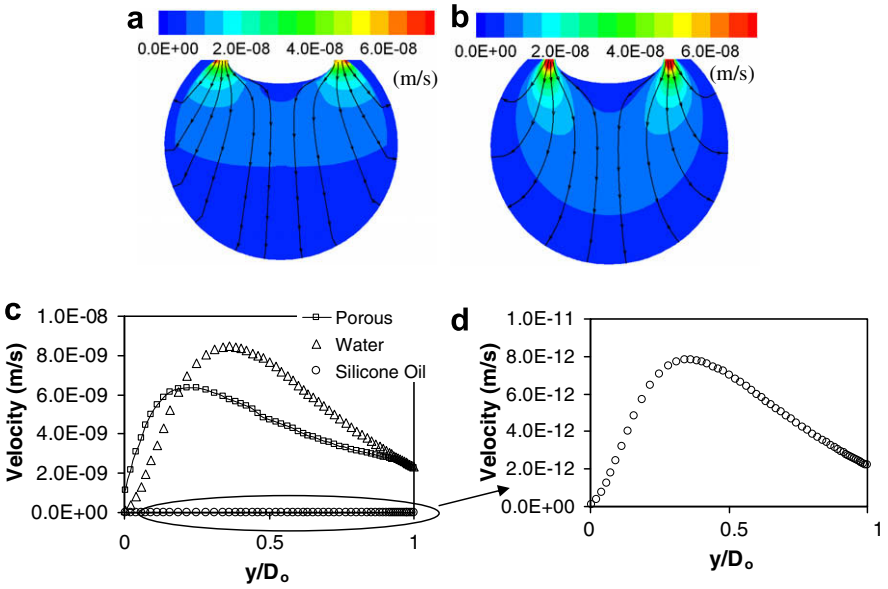

Fig. 5. Velocity magnitude plots: (a,b) contour plot of velocity magnitudes for vitreous modeled as (a) porous medium, (b) liquid (water), (c) velocity along the center-line of the vitreous chamber, (d) zoomed view of the encircled region in Fig. 5c.

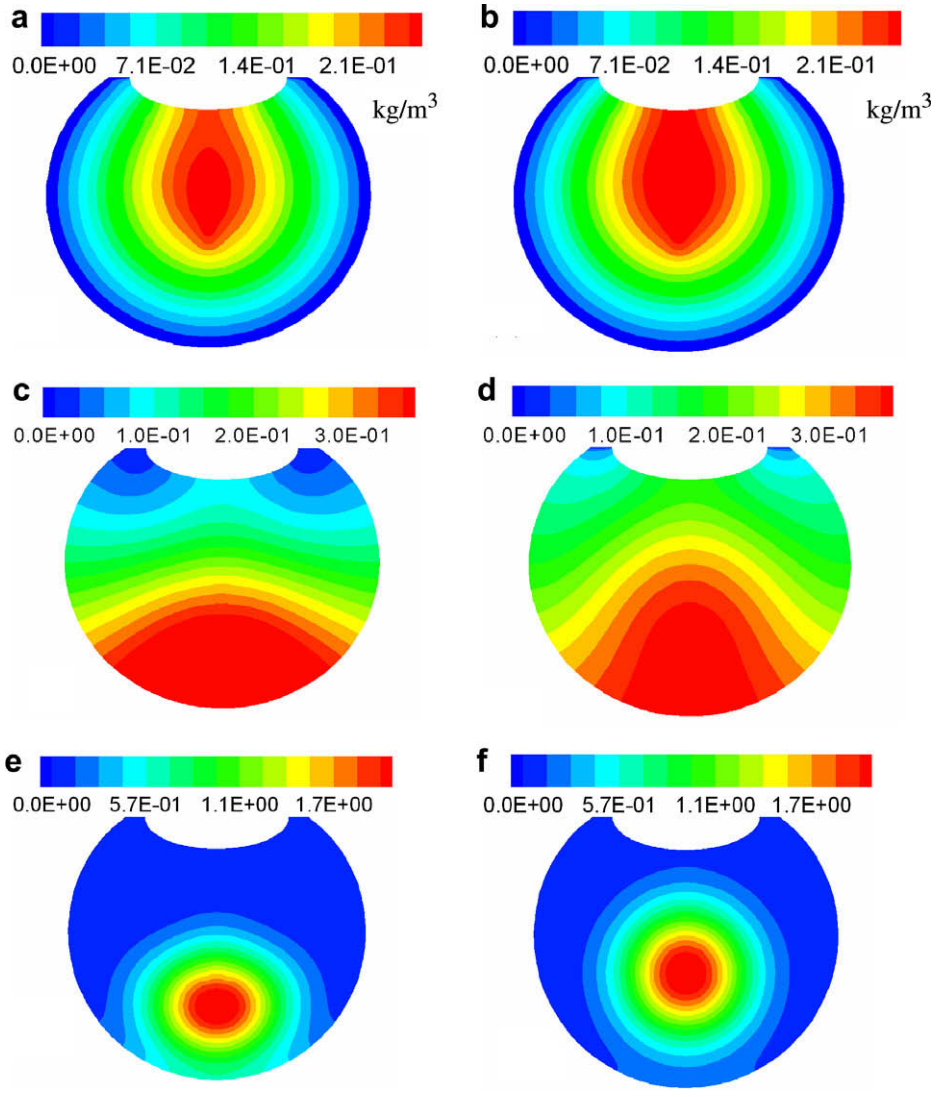

Fig. 6. Concentration contours at time $t = 100$ h: (a) water for $D = 6e{-}10$ m^2/s, (b) silicone oil for $D = 6e{-}10$ m^2/s, (c) water for $D = 3.9e{-}11$ m^2/s, (d) silicone oil for $D = 3.9e{-}11$ m^2/s, (e) water for $D = 1e{-}11$ m^2/s and (f) silicone oil for $D = 1e{-}11$ m^2/s.

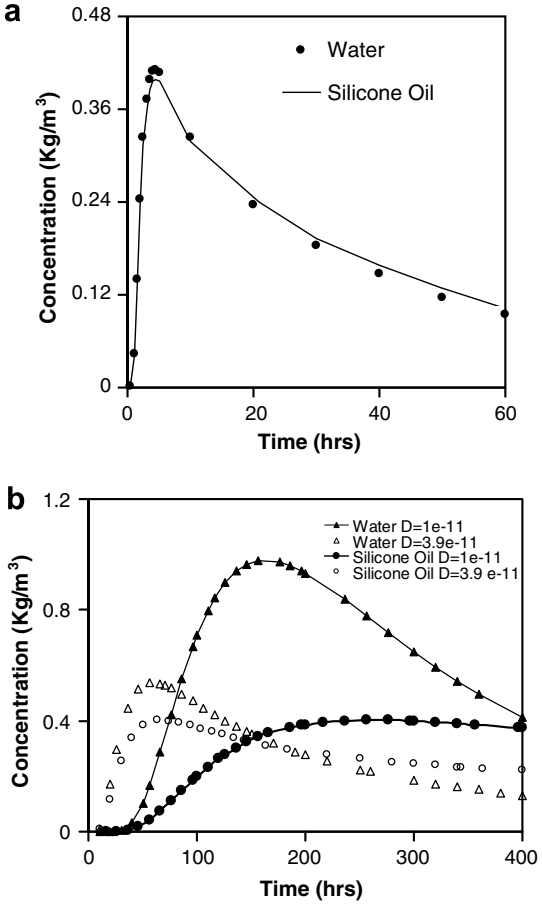

Fig. 7. Concentration plot at the center of the retinal surface: (a) $D = 6e{-}10\ m^2/s$ and (b) $D = 3.9e{-}11\ m^2/s$ and $D = 1e{-}11\ m^2/s$.

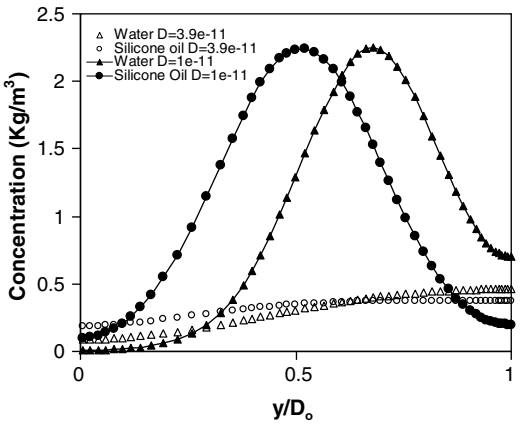

Fig. 8. Concentration line plot along the center of the vitreous chamber at $t = 100$ h.

reaches the highest value of 0.5373 kg/m^3 at about $t = 56$ h whereas for lower diffusion coefficient drugs $D = 1e{-}11\ m^2/s$ the drug reaches the maximum concentration of 0.979 kg/m^3 at time $t = 166$ h. Here it is seen that with decrease in the diffusion coefficient by a factor of about four, the time required to reach the maximum concentration increases by 66% while the peak concentration level at the bottom of the retinal surface increases by 45%. Similarly, for silicone oil with $D = 3.9e{-}11\ m^2/s$, the concentration of the drug reaches the highest value of 0.4012 kg/m^3 at time $t = 64$ h whereas for lower diffusion coefficient drug i.e., $D = 1e{-}11\ m^2/s$ the drug reaches the maximum concentration of 0.4024 kg/m^3 at time $t = 256$ h. For the case of silicone oil there is no increase in the peak concentration but the time required for the drug to reach the maximum concentration increases by 75%.

The higher decay rates for water reflect the greater role of convection in this case. In contrast, the time required to reach the peak retinal concentrations for silicone oil is increased by a factor of approximately 1.5. Therefore, drug-retention in the vitreous chamber is significantly enhanced with silicone vitreous substitutes. These significantly different drug distributions in space and time for different vitreous fluids underscore the relative importance of understanding drug-vitreous fluid interactions before making decisions on appropriate therapy.

Fig. 8 shows the concentration plot along the center-line of the vitreous chamber at $t = 100$ h. The peak concentration of the drug with $D = 3.9e{-}11\ m^2/s$ is shifted towards the retinal surface ($y/D = 1$) whereas for drugs with $D = 1e{-}11\ m^2/s$ the peak concentration of the drug has still not reached the retinal surface. For drugs with $D = 1e{-}11\ m^2/s$, the peak concentration is closer to the retinal surface with water as the vitreous fluid indicating the greater role of convection. This observation can be analyzed using the Péclet number defined as $Pe = \frac{v}{D/d}$ where v is the average velocity along the centre of vitreous chamber, d is the characteristic length, and D is the diffusivity of the drug in the vitreous. A Péclet number greater than one indicates that transport by pressure-induced convective flow is important. For water with $D = 1e{-}11\ m^2/s$, the Péclet number is 12.54, indicating that convection is the primary mode of drug delivery. For silicone oil with $D = 1e{-}11\ m^2/s$, the Péclet number is about 0.012 which indicates that diffusion is the primary mode of drug delivery.

Fig. 9 shows the concentration of the drug along the circumferential surface of the retinal surface at $t = 10$ h. As the problem is symmetrical, the results are plotted only for the one half section of the retinal surface. For water and silicone oil, with drug diffusion

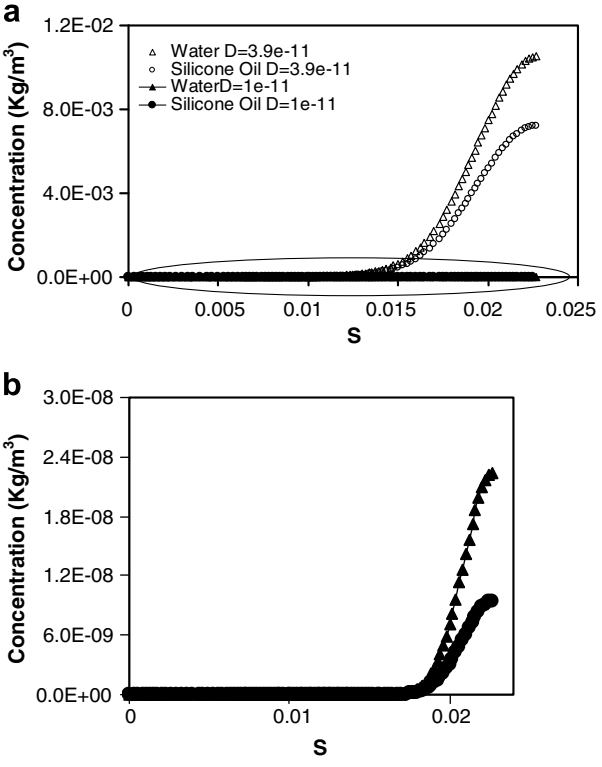

Fig. 9. (a) Concentration line plot along the circumference of retinal surface at time $t = 10$ h and (b) zoomed view of the encircled region in Fig. 9a.

coefficient $D = 3.9e{-}11\ m^2/s$, the drug expectedly provides better circumferential coverage compared to the drug with lower diffusion coefficient. As seen, concentrations are highest at the center of the retinal surface, but approximately 6% of the peak concentration of the drug reaches the anterior portion of retinal surface i.e., at $S = 0$. For the case of $D = 1e{-}11\ m^2/s$, the diffusional transport is lower, and there is approximately six orders of decrease in magnitude of the drug concentration reaching the retinal surface at $t = 10$ h.

Fig. 10 shows the concentration of the drug along the circumferential surface of the retinal surface at $t = 100$ h. Due to the increased role of convection with water, increased amount of drug reaches the retinal surface – it is 18% greater for the higher diffusion coefficient and nearly three times greater for the lower diffusion coefficient drug. For silicone oil, due to the dominance of diffusion, it is seen that approximately 68% more amount of drug reaches the anterior surface of retina when compared to water as vitreous substitute. When comparing the amount of drug reaching the anterior surface of the retina, the concentration is approximately zero for drugs with $D = 1e{-}11\ m^2/s$. This implies that higher diffusion coefficient drugs are more suitable if therapy is needed in the anterior portion of the retinal surface.

Table 2 shows the concentration of the drug at the center of retinal surface with respect to time for water with drugs with different diffusion coefficient. A decrease in the drug diffusion coefficient increases the effects of convection and there is an increase in amount of drug reaching the retinal surface. For low diffusion coefficient drugs, it is seen that there is approximately 45% increase in the peak concentration reaching the retinal surface.

Table 3 shows the peak concentration of the drug at the center of retinal surface and the associated time, for silicone oil as the vitreous and for drugs with different diffusion coefficients. As the diffusion coefficient of drug in silicone oil is unavailable, simulations for range of values of diffusion coefficient are carried out (i.e., from $6e{-}10\ m^2/s$ to $1e{-}12\ m^2/s$). For silicone oil, as *Pe* number is less than 1, diffusion is the dominant mode of drug distribution. It is seen in Table 3 that the peak concentration reaching the retinal surface is approximately constant for the different drug diffusivities, but for lower diffusion coefficient drugs, it takes longer to reach the peak value. This relationship between the diffusion coefficient (expressed as a Schmidt number $Sc = \frac{\mu}{\rho \cdot D}$) 'and time taken to reach the peak value is linear as shown in Fig. 11.

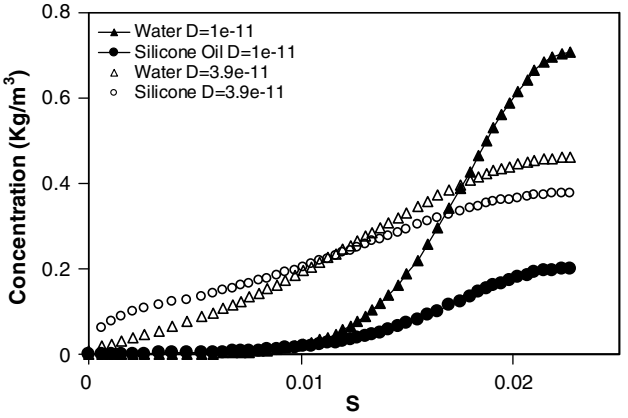

Fig. 10. Concentration line plot along the circumference of retinal surface at time $t = 100$ h.

Table 2
Maximum concentration and the corresponding residence time (water)

D (m^2/s)	C (kg/m^3)	t (h)
6e−10	0.41122	4.6
3.9e−11	0.5373	56
1e−11	0.979	166

D = diffusion coefficient of the drug, C = maximum concentration reaching the centre of the retina and t = time required to reach the maximum concentration.

Table 3
Maximum concentration and the corresponding residence time (silicone oil)

D (m^2/s)	C (kg/m^3)	t (h)
6e−10	0.3985	4.5
3.9e−11	0.4012	64
1e−11	0.4024	256
6e−12	0.4029	436
1e−12	0.405	2410

D = diffusion coefficient of the drug, C = maximum concentration reaching the centre of the retina and t = time required to reach the maximum concentration.

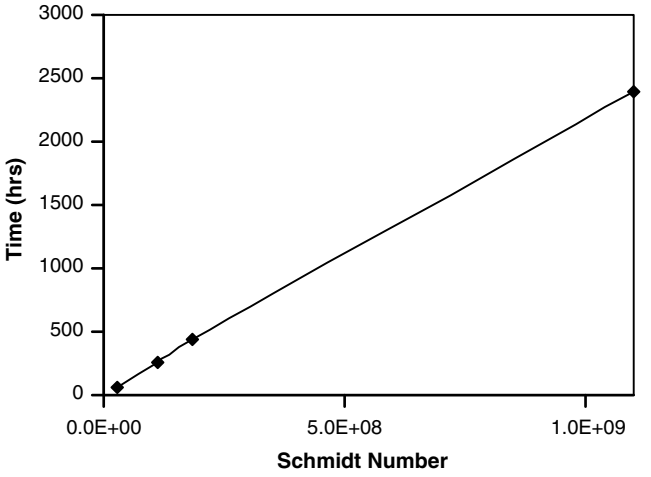

Fig. 11. Schmidt number vs time (Silicone oil).

4.3.2. Time-released drug injection

Attention is turned next to the case where the drug is released as a function of time from a pre-defined volume, as shown in Fig. 1b. The goal with time-released injection is to achieve non-toxic drug concentration levels on the retinal surface, and relatively quickly, so that therapy is initiated shortly after drug injection, and to sustain suitable levels of retinal concentrations over reasonable time duration to maximize the benefit of the initial injection. In evaluating the time-released injection technique, we will make comparisons with the direct injection technique discussed in the previous section. In both cases, the same volume of drug was injected to enable this comparison.

Fig. 12 shows the concentration contours of the drugs with the higher diffusion coefficient, $D = 6e{-}10\ m^2/s$, when injected into water and silicone oil. In this case, transport rates are lower because of the lower release rate, and therefore compared to Fig. 6, the concentration distributions are more localized. The concentration lines are parallel to the retinal surface indicating the important role of the diffusional flux. Due to lower retinal permeability for large molecule drugs, as seen in Fig. 12c–f, the concentration contour lines are nearly perpendicular to both retina and lens boundaries along their entire length. This indicates that the diffusional flux across these surfaces (retina and lens) are small; however, the concentration contour lines are almost parallel to the hyaloid membrane (not evident in Fig. 12 due to the contour levels plotted), indicating that the diffusional flux is normal to this tissue. At $t = 300$ h, Fig. 12c and e shows that for water, significant

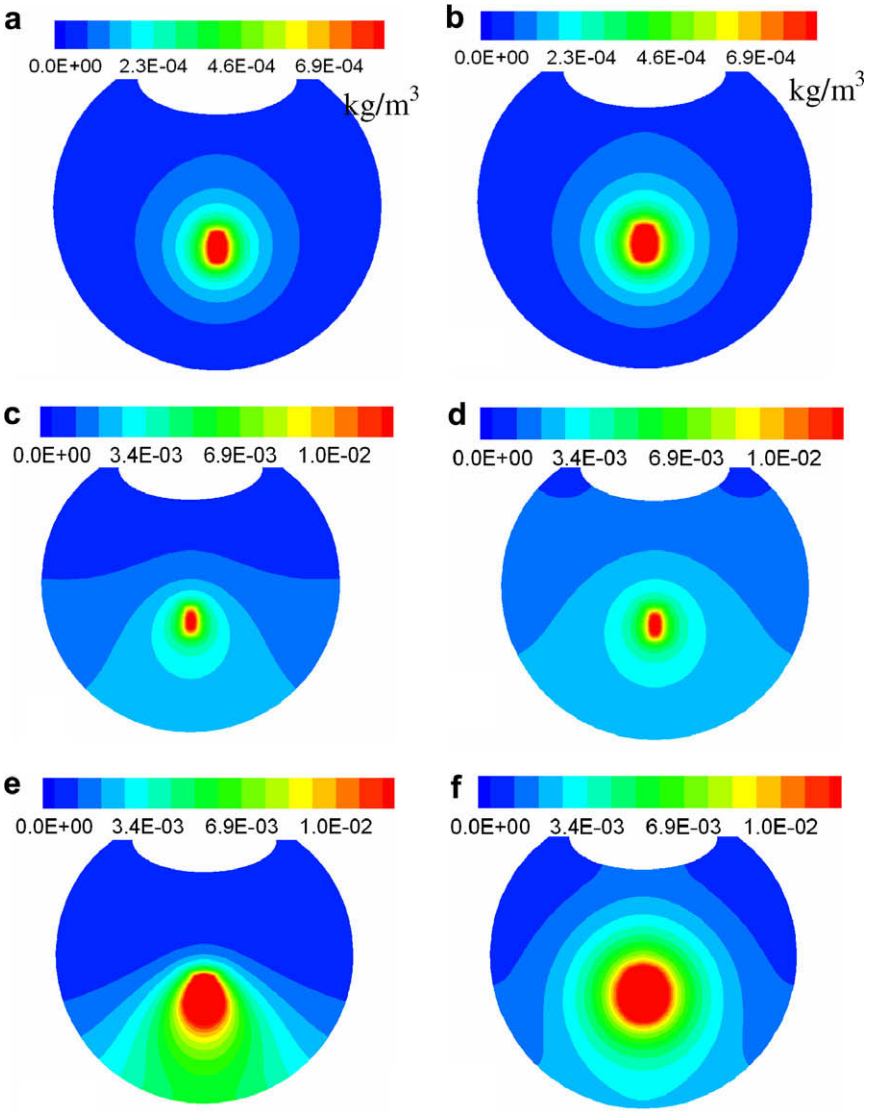

Fig. 12. Concentration contours at time $t = 300$ h: (a) water for $D = 6e{-}10$ m^2/s, (b) silicone oil for $D = 6e{-}10$ m^2/s, (c) water for $D = 3.9e{-}11$ m^2/s, (d) silicone oil for $D = 3.9e{-}11$ m^2/s, (e) water for $D = 1e{-}11$ m^2/s and (f) silicone oil for $D = 1e{-}11$ m^2/s (time-released delivery).

portions of the drug concentration have reached the lower retinal surface and the concentration levels have diminished or disappeared in the upper half of the vitreous chamber. This, in turn, implies the importance of convection effects in water as the vitreous, and that nearly all the drug is transported through the lower portion of the retinal surface. In Fig. 12d and f, it is seen that for silicone oil, the peak concentration of drug is still at the drug injection site (due to the lower convective transport rates for the higher viscosity silicone oil), and that the iso-concentration lines are more circular (indicative of the greater importance of diffusion).

Fig. 13a shows the plot for the concentration of the high diffusion coefficient drug at the center of the retinal surface with respect to time for water and silicone oil. These results are consistent with those shown in Fig. 7 for direct injection, except that the time taken to reach the peak is longer and is nearly 2.8 days (67 h) instead of the 4.6 h for direct injection. Further, the decay rate of the retinal drug concentration is reduced considerably with the time-released option. Thus, the residence time of the drug is longer (factor of 14.8) with bio-degradable drugs compared to the case of direct injection. When compared to direct injection, the peak concentration levels are substantially smaller with the time-released injection with water as the vitreous. Thus, when controlled quantity of the drug is required on the retinal surface over an extended period of time, the time-released drug delivery is the desired option. Because of slower transport rates in the case of silicone oil it is seen in Fig. 13a that peak concentrations of the drug are higher (by 4%), and decay rates are lower when compared to the case of water. For low diffusion coefficient drugs, it can be seen that for water with $D = 3.9e{-}11$ m^2/s (Fig. 13b), the drug reaches the peak concentration of 0.00224 kg/m^3 at $t = 216$ h whereas for $D = 1e{-}11$ m^2/s, the peak concentration attained is 0.005456 kg/m^3 at $t = 316$ h. Compared to direct injection for $D = 3.9e{-}11$ m^2/s, residence times with time-released injection is about 3.8 times longer with water as the vitreous fluid whereas for the drugs with $D = 1e{-}11$ m^2/s the residence time is 1.9 times longer. In contrast, as noted earlier, for the higher diffusion drug, residence times were nearly 14.8 times longer with time-released injection. Therefore, the long residence time benefits of time-released injection decrease for lower diffusion coefficient drugs.

Fig. 14 shows the drug concentration along the center of the vitreous chamber at $t = 400$ h. The peak concentration has still not reached the retinal surface since the drug is released slowly. The high concentration region in the center (in contrast to Fig. 8 with

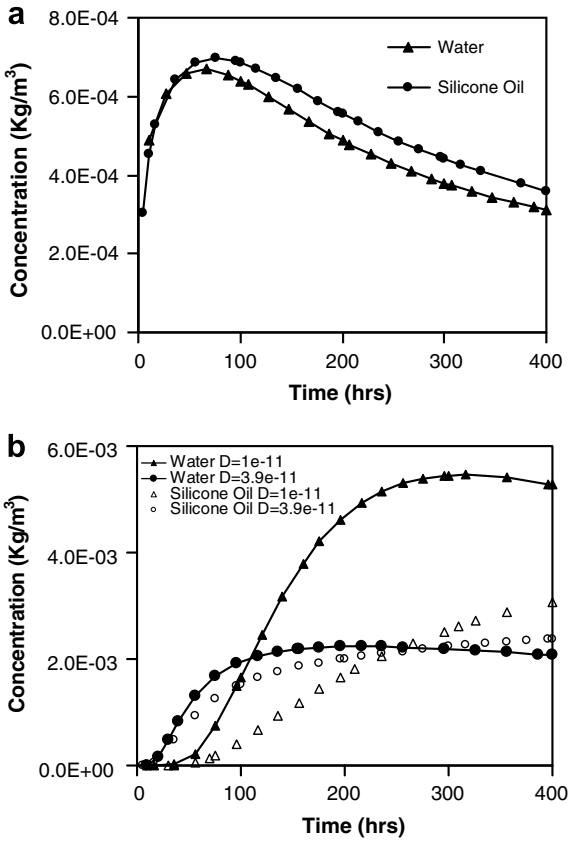

Fig. 13. Concentration plot at the center of the retinal surface: (a) $D = 6e{-}10\ m^2/s$ and (b) $D = 3.9e{-}11\ m^2/s$ and $D = 1e{-}11\ m^2/s$.

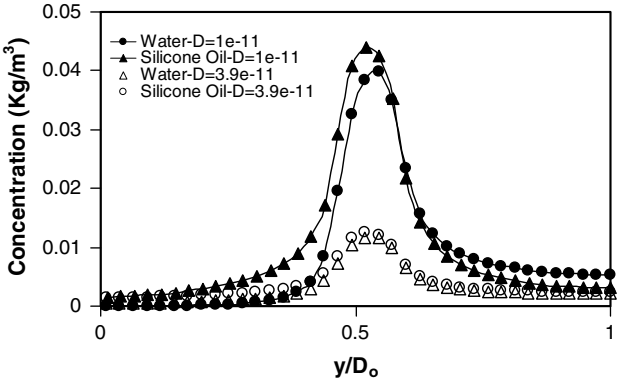

Fig. 14. Concentration line plot along the center of the vitreous chamber at $t = 400$ h.

direct injection) is a reflection of the time-released injection process. At this time, a portion of the drug is still at the injection site or has been just released. As seen in Fig. 14, for drugs with $D = 1e{-}11\ m^2/s$ for water a lesser amount of drug is available at the drug injection position compared to silicone oil, as more of the drug is swept away from the retinal surface due to increased effects of convection.

Fig. 15 shows the drug concentration along the retinal surface at $t = 100$ h. It is seen from the plot that the peak concentration for drugs with $D = 3.9e{-}11\ m^2/s$ with water as vitreous substitute is maximum followed by the drugs with $D = 1e{-}11\ m^2/s$. Moreover, it is seen that for drugs with lower diffusion coefficient i.e., $D = 1e{-}11\ m^2/s$, the amount of drug reaching the anterior portion of retina is approximately zero.

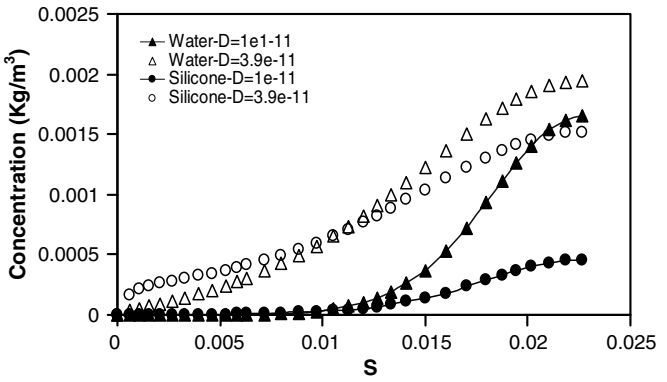

Fig. 15. Concentration line plot along the circumference of retinal surface at time $t = 100$ h.

Fig. 16 shows the drug concentration along the retinal surface at $t = 400$ h. As seen, for drugs with $D = 1e{-}11\ m^2/s$, for water as vitreous substitutes, there is a 41% increase in the amount of the drug reaching the retinal surface compared to silicone oil. For drugs with $D = 1e{-}11\ m^2/s$, due to higher effects of convection only 0.004% of drug reaches the anterior portion of retina. This implies that lower diffusion coefficient drugs are more suitable if therapy is needed primarily in the posterior portion of the retinal surface. Moreover, for silicone oil with $D = 1e{-}11\ m^2/s$, due to higher effects of diffusion, 9% of the drug reaches the anterior portion of retina and for drugs with $D = 3.9e{-}11\ m^2/s$, 17% of the drug reaches the anterior portion of retina. This implies that higher

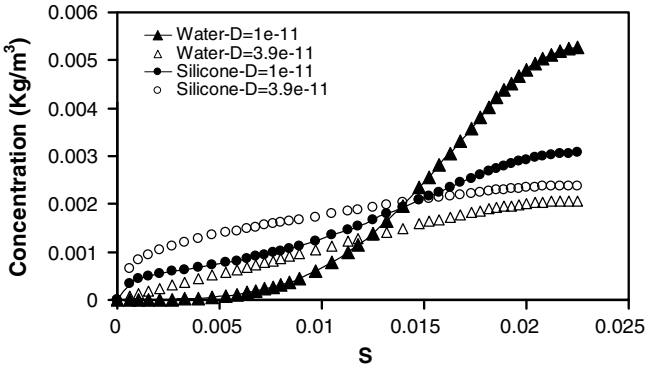

Fig. 16. Concentration line plot along the circumference of retinal surface at time $t = 400$ h.

Table 4
Maximum concentration and the corresponding residence time

Fluid	Injection type	D (m^2/s)	C (kg/m^3)	t (h)
Water	Direct	6e−10	0.4112	4.6
		3.9e−11	0.5373	56
		1e−11	0.979	166
	Time-released	6e−10	6.69e−4	67
		3.9e−11	2.24e−3	216
		1e−11	0.0054	316
Silicone Oil	Direct	6e−10	0.3985	4.5
		3.9e−11	0.4012	64
		1e−11	0.4024	256
	Time-released	6e−10	6.9e−4	76
		3.9e−11	8.3e−4	810
		1e−11	4.48e−3	3480

D = diffusion coefficient of the drug, C = maximum concentration reaching the centre of the retina and t = time required to reach the maximum concentration.

diffusion coefficient drugs are more suitable if therapy is needed in the anterior portion of the retinal surface.

The results of the simulations carried out are summarized in Table 4. It is seen that in time-released drug injection, where the drug is released as a function of time, drug concentration levels are several orders of magnitudes lower than those of direct injection, and dangers of retinal toxicity are avoided. Further, drug residence times are considerably longer with time-released injection, being nearly 10–12 times greater for the higher diffusion coefficient drug. In the case of direct injection of drugs with low diffusion coefficient, the peak concentration levels of 0.979 kg/m^3 for water with $D = 1e{-}11$ m^2/s is quite high, and potentially can lead to retinal toxicity.

5. Concluding remarks

A three-dimensional computational strategy was developed to investigate drug delivery in eyes after undergoing vitrectomy. The geometrical model adopted uses a realistic representation of the retina and the sclera (modeled as porous layers with specific hydraulic permeability), and predictions are obtained for both the flow-field and the drug concentrations by solving the conservation equations for mass, momentum and drug concentrations. Results are presented for water and silicone oil as the vitreous fluid. Two drug delivery techniques are considered: (a) direct injection, where the injected drug is released instantaneously into the vitreous and (b) time-released injection of a drug, where the drug is released in a specified time-dependent manner. The following are the major conclusions of the present study:

(1) The concentration distribution depends on the vitreous fluids, permeability of retina and the diffusion coefficient of the drug.
(2) Water as vitreous fluids exhibit higher drug transport rates than silicone oil. This observation was related to convection effects that play a more important role in the case of water. For silicone oil, convection effects are smaller due to the higher viscosity, and diffusion is more important.
(3) In the case of direct injection, for water as vitreous fluid, the retinal drug concentration levels reach high values, even for low diffusivity drugs, and such situations can lead to retinal toxicity.
(4) For drugs with high diffusion coefficient (and retinal permeability), a more uniform distribution of the drug is obtained along the surface of the retina whereas for the low diffusion coefficient drugs the concentration of drug is localized along the posterior surface of the retina.
(5) Time-released injection is shown to provide considerably lower levels of drug concentration along the retinal surface for sustained periods of time. This is likely to reduce the local toxicity arising from high drug concentrations, and to provide sustained therapy over a longer period of time compared to direct injection.
(6) For low diffusion coefficient drugs, due to higher effects of convection, and reduced retinal permeability, the amount of drug reaching the anterior portion of retina is approximately zero. This implies that higher diffusion coefficient drugs are more suitable if therapy is needed in the anterior portion of the retinal surface.

Acknowledgements

This work was supported by a grant from the Louisiana Health Excellence Fund through the Biological Computation and Visualization Center (BCVC). This support is gratefully acknowledged.

References

[1] D.H. Geroski, H.F. Edelhauser, Drug delivery for posterior segment of eye disease, Invest. Ophthal. Vis. Sci. 41 (2000) 961–964.
[2] D. Maurice, Review: practical issues in intravitreal drug delivery, J. Ocul. Pharmacol. Therap. 17 (2001) 393–401.
[3] M. Araie, D.M. Maurice, The loss of fluorescein, fluorescein glucuronide and fluorescein isothiocyanate dextran from the vitreous by the anterior and retinal pathways, Exp. Eye Res. 52 (1991) 27–39.
[4] K.J. Tojo, A. Ohtori, Pharmacokinetic model of intravitreal drug injection, Math. Biosci. 123 (1994) 59–75.
[5] S. Friedrich, Y. Cheng, B. Saville, Finite element modeling of drug distribution in the vitreous humor of the rabbit eye, Ann. Biomed. Eng. 25 (1997) 303–314.
[6] S. Friedrich, Y. Cheng, B. Saville, Drug distribution in the vitreous humor of the human eye: the effect of intravitreal injection position and volume, Curr. Eye Res. 16 (1997) 663–669.
[7] J. Xu, Controlled release and the concentration distribution of the drug in the vitreous humor, M.S. Thesis, University of Colorado, CO, 1999.
[8] M.S. Stay, J. Xu, T.W. Randolph, V.H. Barocas, Computer simulation of convective and diffusive transport of controlled-release drugs in the vitreous humor, Pharmaceut. Res. 20 (2003) 96–102.
[9] P. Missel, Hydraulic flow and vascular clearance influences on intravitreal drug delivery, Pharmaceut. Res. 19 (2002) 1636–1647.
[10] J. Park, P.M. Bungay, R. Lutz, J. Augsburger, R. Millard, A. Roy, et al., Evaluation of coupled convective–diffusive transport of drugs administrated by intravitreal injection and controlled release implant, J. Contr. Release 105 (2005) 279–295.
[11] M.J. Colthrust, R.L. Williams, P.S. Hiscott, I. Grierson, Biomaterials used in the posterior segment of the eye, Biomaterials 21 (2000) 649–665.
[12] G. Stainer, G.A. Peyman, H. Meisels, G. Fishman, Toxicity of selected antibiotic in vitreous replacement fluid, Ann. Ophthal. 9 (1977) 615–618.
[13] H.M. Hegazy, M. Kivilcim, G.A. Peyman, M.H. Unal, C. Liang, L.C. Molinari, A.A. Kazi, Evaluation of toxicity of intravitreal ceftazidime, vancomycin, and ganciclovir in a silicone oil-filled eye, Retina 19 (1999) 553–557.
[14] G. Eisner, The anatomy and biomicroscopy of the vitreous body, in: Documenta Ophthalmologica Proceedings Series, New Develop. Ophthalmol. (1974) 87–104.
[15] J.P. L'Huillier, G. Apiou-Sbirlea, Computational modeling of ocular fluid dynamics and thermodynamics, in: Medical Applications of Computer Modeling: Cardiovascular and Ocular Systems, WIT Press, 2000 (Chapter 7).
[16] R.C. Tripathi, B.J. Tripathi, Anatomy of the Human Eye, Orbit, and Adnexa, in: Hugh Davson (Ed.), The Eye, Vegetative Physiology and Biochemistry, Vol. 1a, Academic Press, 1984.
[17] B. Alamouti, B.J. Funk, Retinal thickness decreases with age: an OCT study, J. Ophthalmol. 87 (2003) 899–901.
[18] J. Kaiser, D. Maurice, The diffusion of fluorescein in the lens, Exp. Eye Res. 3 (1964) 156–165.
[19] L. Pitkänen, V. Ranta, V.H. Moilanen, A. Urtti, Permeability of Retinal rigment epithelium: effects of permeant molecular weight and lipophilicity, Invest. Ophthalmol. Vis. Sci. 46 (2005) 641–646.
[20] N. Rashidnia, R. Balasubramaniam, J. Kuang, P. Petitjeans, T. Maxworthy, Measurement of the diffusion coefficient of miscible fluids using both interferometry and wiener method, Int. J. Thermophys. 22 (2001) 547–555.
[21] R.T. Falk, T.W. Randolph, R. Meyer, M. Manning, Controlled release of ionic compound for poly (L-lactide) micro-sphere produced by precipitation with a compressed anti-solvent, J. Contr. Release 44 (1997) 77–85.
[22] C.R. Ethier, M. Johnson, J. Ruberti, Ocular biomechanics and biotransport, Annu. Rev. Biomed. Eng. 6 (2004) 249–273.
[23] M. Gonvers, J. Hornumg, C. Courten, The effect of liquid silicone on the rabbit retina, Arch. Ophthal. 104 (1986) 1057–1062.
[24] S. Ergun, Fluid flow through packed columns, Chem. Eng. Prog. 48 (1952) 89–94.
[25] A. Edwards, M.R. Prausntiz, Fiber matrix model of sclera and corneal stroma for drug delivery to the eye, AIChE 44 (1998) 214–225.
[26] I. Fatt, Flow of water in the sclera, Exp. Eye Res. 10 (1970) 243–249.
[27] http://www.fluentusers.com/fluent/doc/ori/html/ug/main_pre.htm.
[28] J.P. Vandoormaal, G.D. Raithby, Enhancement of the SIMPLE method for predicting incompressible fluid flows, Numer. Heat Transf. 7 (1984) 147–163.
[29] S. Friedrich, B. Saville, Y.L. Cheng, Drug distribution in the vitreous humor of the human eye: the effects of aphakia and changes in retinal permeability and vitreous diffusivity, J. Ocul. Pharmacol. Ther. 13 (1997) 445–459.
[31] C.M. Germillion, G.A. Peyman, K. Lui, K. Naguib, Fluorosilicone oil in the treatment of retinal detachment, Br. J. Ophthal. 74 (1990) 643–646.